Resilience assessment for interdependent urban infrastructure systems using dynamic network flow models

Nils Goldbeck*

Centre for Transport Studies, Department of Civil and Environmental Engineering, Imperial College London, Skempton Building, London SW7 2AZ, United Kingdom, n.goldbeck14@imperial.ac.uk

Panagiotis Angeloudis

Centre for Transport Studies, Department of Civil and Environmental Engineering, Imperial College London, Skempton Building, London SW7 2AZ, United Kingdom, p.angeloudis@imperial.ac.uk

Washington Y Ochieng

Centre for Transport Studies, Department of Civil and Environmental Engineering, Imperial College London, Skempton Building, London SW7 2AZ, United Kingdom, w.ochieng@imperial.ac.uk

*Corresponding author

Abstract:

Critical infrastructure systems in cities are becoming increasingly interdependent, therefore exacerbating the impacts of disruptive events through cascading failures, hindered asset repairs and network congestion. Current resilience assessment methods fall short of fully capturing such interdependency effects as they tend to model asset reliability and network flows separately and often rely on static flow assignment methods. In this paper, we develop an integrated, dynamic modelling and simulation framework that combines network and asset representations of infrastructure systems and models the optimal response to disruptions using a rolling planning horizon. The framework considers dependencies pertaining to failure propagation, system-of-systems architecture and resources required for operating and repairing assets. Stochastic asset failure is captured by a scenario tree generation algorithm whereas the redistribution of network flows and the optimal deployment of repair resources are modelled using a minimum cost flow approach. A case study on London's metro and electric power networks shows how the proposed methodology can be used to assess the resilience of city-scale infrastructure systems to a local flooding incident and estimate the value of the resilience loss triangle for different levels of hazard exposure and repair capabilities.

Keywords: Resilience assessment, interdependent infrastructure systems, infrastructure assets, repairable systems modelling, dynamic network flow modelling

1. INTRODUCTION

Various disasters in recent years have brought to light critical infrastructure vulnerabilities linked to interactions between different systems. For example, the disruptions caused by superstorm Sandy in New York City in 2012 were aggravated by various incidents of cascading failure [1]. Extensive power outages made it more difficult to remove flood water from metro tunnels [2]. The liquid fuel supply chain broke down due to direct flood damage to terminals, refineries and pipelines, combined with power outages and traffic restrictions on the waterways [3]. The fuel shortage, in turn, affected emergency response services and efforts to restore power supply. Similar interactions have been documented for other disasters, including the 1998 ice storm in Canada [4], 2008 winter storms in China [5], 2010 earthquake in Chile [6], and 2010/2011 earthquakes in New Zealand [7].

The interplay of different infrastructure systems can equally exacerbate impacts of much smaller trigger events. In 2015, a fire started in an underground electrical substation in London and damaged a natural gas pipeline, which in turn fuelled the fire for 36 hours [8]. Despite being a relatively local incident, it resulted in high costs for businesses due to disruptions in power, communication and transport systems.

These examples demonstrate that the state of a critical infrastructure system can be affected by disruptions in other systems through different types of dependency relations. Systems that are mutually dependent on each other are referred to as interdependent infrastructure systems or a system-of-systems. Rinaldi et al. [9] were among the first to highlight the trend of increasing infrastructure interdependency and expressed concern that assessing the performance of each system separately could be misleading because important interdependency effects are not taken into account. The issue has since gained the attention of many researchers, government authorities and industry practitioners, especially in conjunction with the emerging concept of infrastructure resilience.

Traditional risk management strategies provide plans to avoid, control, transfer or assume risks based on assessing their probability and impact. The applicability of such methods is limited when there is high uncertainty regarding the risk matrix and effectiveness of control or avoidance measures. This is increasingly the case for urban infrastructure systems, and the concept of infrastructure resilience extends risk management efforts accordingly. Infrastructure resilience describes the ability of systems to resist, recover and adapt in order to maintain their core function after a perturbation (for a comprehensive review of definitions see [10]). As such, resilience approaches seek to understand the dynamic behaviour of systems on different timescales and optimise both preparedness and recovery capabilities. As this dynamic behaviour is increasingly determined by interdependencies, new methods are needed to model urban infrastructure as a system-of-systems and carry out comprehensive resilience assessments.

Qualitative studies in this field have provided definitions and typologies of infrastructure dependencies (e.g. [9], [11], [12]). Several quantitative methods have been developed or adapted to

analyse the resilience of interdependent infrastructure systems, including fault tree analysis [13], system dynamics [14], agent-based simulation [15], input-output modelling [16], and network modelling [17]–[24]. Comprehensive reviews of such methods are provided by Ouyang [25] and Iturriza et al. [26]. Regarding priorities for future research, Ouyang [25] and Zio [27] highlight the importance of model integration and co-simulation.

Modelling approaches using network science broadly fall into two categories: topological models and flow models. Topological models (e.g. [17], [19], [21], [24]) show that interdependencies are a source of additional vulnerabilities and can aid network collapse. However, topological models only analyse network structure and fail to capture fundamental aspects of infrastructure networks beyond connectivity, for example, partial capacity loss, routing and congestion. Previous studies have shown that more realistic vulnerability and resilience assessments can be achieved with network flow models, which seek to predict the flow of passengers, goods, power or information, taking into account the capacity of different network components and other operational network characteristics [28]–[32]. The network flow models proposed by Lee II et al. [18], Holden et al. [20], Jin et al. [22] and Fotouhi et al. [23] are particularly relevant to this paper, given their ability to capture interdependent networks. Key features of these models are presented in Table 1.

Table 1 Key features of network flow models for interdependent urban infrastructure systems

	Lee II et al. [18]	**Holden et al.** [20]	**Jin et al.** [22]	**Fotouhi et al.** [23]
Case study area	New York City	n.a.	Singapore	Minneapolis
Networks considered	• Metro • Electric power • Telephone	• Water • Electric power	• Metro • Bus	• Road • Electric power
Single-commodity networks	✓	✓		(✓)
Multi-commodity networks	✓		✓	✓
Network size	100 - 1000 nodes	6 nodes	77 nodes	8 nodes
Resilience measure	Total cost (incl. penalty for unmet demand)	Satisfied demand	Satisfied demand	Total travel time
Min. cost flow assignment	✓	✓	✓	✓
Dynamic flows		✓		
Coupling of flows	✓	✓	✓	
Partial capacity loss		continuous		discrete
Mitigation	Temporary power and telephone connections		Replacement bus services	Backup power supply, traffic regulation by police officers
Repair				✓
Integer variables	✓		✓	✓
Nonlinear constraints				✓
Stochastic optimisation			✓	✓

A common feature found across most state-of-the-art network flow models is their use of minimum cost flow methods to assign flows to capacitated networks, with differences in the representation of flow relationships between different networks. For instance, Holden et al. [20] use a linear production

function that defines the quantities of input resources required for the production of another good. Fotouhi et al. [23] add delays to road links if traffic signals fail, depending on whether the junctions are subsequently unregulated or regulated manually by police officers. While such modelling techniques achieve tailor-made solutions to capture specific aspects of infrastructure systems, a more generic approach is needed that can represent the many different interactions between network flows and physical infrastructure assets.

In existing network flow models, infrastructure assets, such as metro stations, railway tracks or electricity substations, are often modelled as simple nodes or links whose operational characteristics are condensed into one-dimensional operability variables. Moreover, these operability variables are usually exogenous or subject to a simple stochastic process (random failure). In reality, such infrastructure assets are complex systems themselves, consisting of sub-systems and components. The realism of network flow models could be improved by modelling the multi-level architecture of infrastructure assets, for example using the reliability engineering concept of series and parallel systems.

With recovery time being a core resilience dimension, resilience assessment methods are required to model the dynamic behaviour of interdependent infrastructure systems. The two-stage stochastic programming methods proposed in Jin et al. [22] and Fotouhi et al. [23] consider decisions taken at two points in time (before and after the disruption), but the actual flow assignment is static. In Holden et al. [20], the static flow assignment is repeated over a series of time steps. However, none of the reviewed models features a dynamic flow assignment where flows can span over multiple time steps. Moreover, there exists currently no models that capture the dynamic interplay of network flows and asset operability during the recovery period.

The optimisation problems in the reviewed models are either inherently linear or linearly approximated. However, they often include binary variables and, therefore, belong to the class of NP-hard computational problems. We note that most case studies presented in the literature involve network instances featuring fewer than 100 nodes, with the exception of the New York City example in Lee II et al. [18]. City-scale infrastructure networks are at least one order of magnitude larger. While in some cases it may be practical to assess or optimise resilience considering only a smaller local area, there is also a need for models that are scalable to full-size urban infrastructure networks.

Summarising, this paper seeks to address three gaps in the literature: i) lack of methods to represent infrastructure assets in network flow models more realistically and capture the relationship between network flows and asset operability, ii) insufficient modelling of dynamic effects during the recovery period, and iii) limited scalability. The remainder of the paper is structured as follows. Section 2 presents resilience measures. Section 3 introduces the modelling framework, including four types of dependency relations. Section 4 presents the integrated asset operability and network flow model. The application of the method is demonstrated in a case study on London in Section 5.

Table 2 Nomenclature

Sets		**Parameters**		**Variables**	
A	Infrastructure assets	$t_{\max}$	Number of simulation timesteps	$Z_{k,m}^{t}$	Random variable for failure propagation
A^{S}	Series systems assets	t_{ph}	Length of the planning horizon	z_k^t	Asset failure variable for k
A^{P}	Parallel systems assets	n_{scn}	Max. number scenarios	x_k^t	Operability of asset k
H	Hazard events	n_{spl}	Number of samples per scenario tree node	y_k^t	Utilisation of asset k
V^{SC}	Nodes in single-commodity systems	k	Number of shortest paths per OD pair	$f_{i,j}^t$	Flow on link (i,j)
V^{MC}	Nodes in multi-commodity systems	$\breve{u}_i^t$	Commodity demand at node i	f_p^t	Flow on path p
E^{SC}	Links in single-commodity systems	$\breve{f}_{o,d}^t$	Travel demand from o to d	g_i^t	Commodity generation at node i
E^{MC}	Links in multi-commodity systems	v_i^{SC}	Value of commodity demand at node i	u_i^t	Commodity delivery at node i
OD	OD pairs	$v_{o,d}^{\mathrm{MC}}$	Value of travel demand from o to d	VoD_t	Value of demand
$P_{o,d}$	Shortest paths from o to d	$\hat{f}_{i,j}$	Capacity of link (i,j)	VoS_t	Value of supply
$Q_{i,j}$	Paths using link (i,j)	$\hat{g}_i$	Capacity of node i	RLT	Area of the resilience loss triangle
D^{F}	Failure propagation dependencies	$c_{i,j}^{\mathrm{f}}$	Cost of flow on link (i,j)	MSP	Minimum system performance
D^{L}	Logic dependencies	c_i^{g}	Cost of commodity generation at node i	TLD	Total length of disruption
D^{U}	Asset utilisation dependencies	$p_{k,m}$	Probability of failure propagation from k to m		
D^{I}	Resource input dependencies	$t_{k,m}$	Time lag of failure propagation from k to m		
		$\alpha_{i,k}^{\mathrm{U}}$	Resources provided by i for the utilisation of k		
		$\alpha_{i,k}^{\mathrm{R}}$	Resources provided by i for the repair of k		

2. RESILIENCE MEASURES

Literature reviews by Hosseini et al. [10] and Sun et al. [33] highlight the existence of several competing measures of infrastructure resilience. One of the most commonly used approaches is the loss triangle method, which quantifies resilience based on the loss of system performance integrated over the time it takes for the system to recover after a disruption [34].

Performance measures used in this context include those that are based on asset operability (e.g. [15], [31], [32], [35]), network connectivity (e.g. [17], [36]–[39]), network capacity (e.g. [40], [41]), satisfied demand (e.g. [15], [22], [24], [31], [32], [42]–[44]), and the value of services provided (e.g. [23], [45]–[50]). In this paper, we use a performance measure based on the value of service provision because it has the following advantages: First, a value-based performance measure is most relevant from a societal perspective, as it captures the quantity and quality of services provided by infrastructure systems to meet a certain demand. Second, it can usually be expressed in monetary values, which facilitates the aggregation of performance measures for different infrastructure systems and services. Third, positive and negative externalities can be integrated in the performance measure by converting them to monetary values. The difficulty of using a value-based performance measure is that more sophisticated prediction models and data inputs are required for its evaluation compared to other performance measures.

We propose a generic performance measure that can be applied to all types of infrastructure systems. Services provided by these systems are of two types: i) the supply of a homogeneous good or service to a set of demand nodes, or ii) the transportation of inhomogeneous goods, passengers or information between origin-destination (OD) pairs. Distinguishing these two types of infrastructure services is important because they require different flow assignment methods, referred to as single- and multi-commodity network assignment.

An overview of the notation used throughout this paper is provided in Table 2. The demand for infrastructure services is assumed to be given by parameters $\check{u}_i^t$ for goods or services required at nodes $i \in V^{\mathrm{SC}}$ in single-commodity networks and $\check{f}_{o,d}^t$ for transportation services between two nodes $(o,d) \in OD$ in multi-commodity networks. In the first instance, our model does not capture demand elasticity, but the framework could be extended in this respect in the future.

We assume that the monetary value of fulfilling one unit of the demand for infrastructure services with a standard quality of service level can be estimated by parameters v_i^{SC} and $v_{o,d}^{\mathrm{MC}}$. The total value of demand (VoD) at time step t can then be calculated as follows:

$$\mathrm{VoD}_t = \sum_{i \in V^{\mathrm{SC}}} v_i^{\mathrm{SC}} \check{u}_i^t + \sum_{(o,d) \in OD} v_{o,d}^{\mathrm{MC}} \check{f}_{o,d}^t \tag{1}$$

When a disruption occurs, it is possible that some of the demand remains unsatisfied. Additionally, there could be a deterioration of service quality. The value of supply (VoS) is calculated as follows:

$$\mathrm{VoS}_t = \sum_{i \in V^{\mathrm{SC}}} \alpha_i^t v_i^{\mathrm{SC}} u_i^t + \sum_{(o,d) \in OD} v_{o,d}^{\mathrm{MC}} \sum_{p \in P_{o,d}} \frac{c_{o,d}}{c_p} f_p^t \tag{2}$$

For a single-commodity node $i \in V^{\mathrm{SC}}$, the value of supply is the quantity supplied u_i^t, multiplied by the value of delivering this commodity v_i^{SC}, and a discount factor $\alpha_i^t \in [0,1]$ indicating the quality of service. Similarly, for an origin destination pair $(o,d) \in OD$, the discount factor applied to path flows f_p^t is $\frac{c_{o,d}}{c_p}$, where $c_{o,d}$ and c_p are the generalised costs of transport between o and d over the shortest path and over the chosen path p respectively.

With the overall system performance measure $\frac{\mathrm{VoS}_t}{\mathrm{VoD}_t}$, we can now calculate the main resilience measure, the area of the resilience loss triangle (RLT), by integrating over all simulation time steps:

$$\mathrm{RLT} = \sum_{t=0}^{t_{\max}} \left(1 - \frac{\mathrm{VoS}_t}{\mathrm{VoD}_t}\right) \tag{3}$$

Two additional measures are used to capture aspects which other studies describe as the robustness and rapidity dimensions of resilience [51]. Robustness can be seen as the minimum system performance:

$$\mathrm{MSP} = \min_{t=0,\ldots,t_{\max}} \left(1 - \frac{\mathrm{VoS}_t}{\mathrm{VoD}_t}\right) \tag{4}$$

The rapidity of recovery is measured by the total length of the disruptions, i.e. the number of time steps where the system performance is less than one:

$$\mathrm{TLD} = \sum_{t=0}^{t_{\max}} \mathbb{1}_{\{x<1\}} \left(\frac{\mathrm{VoS}_t}{\mathrm{VoD}_t}\right) \tag{5}$$

Note that the resilience measures formulated above do not include the costs of infrastructure service provision, which are likely to increase after a disruptive event due to recovery and repair costs. Furthermore, externalities may occur, such as environmental impacts. The network flow modelling method can capture these costs by adding them either to the objective function (e.g. monetised environmental impacts) or as constraints (e.g. repair budgets).

3. METHODOLOGICAL FRAMEWORK

In this section, we present a modelling and simulation framework that can be used to assess the resilience of a system of interdependent infrastructure systems. Figure 1 presents the high-level architecture and the remainder of this section describes how the model represents infrastructure systems and dependency relations.

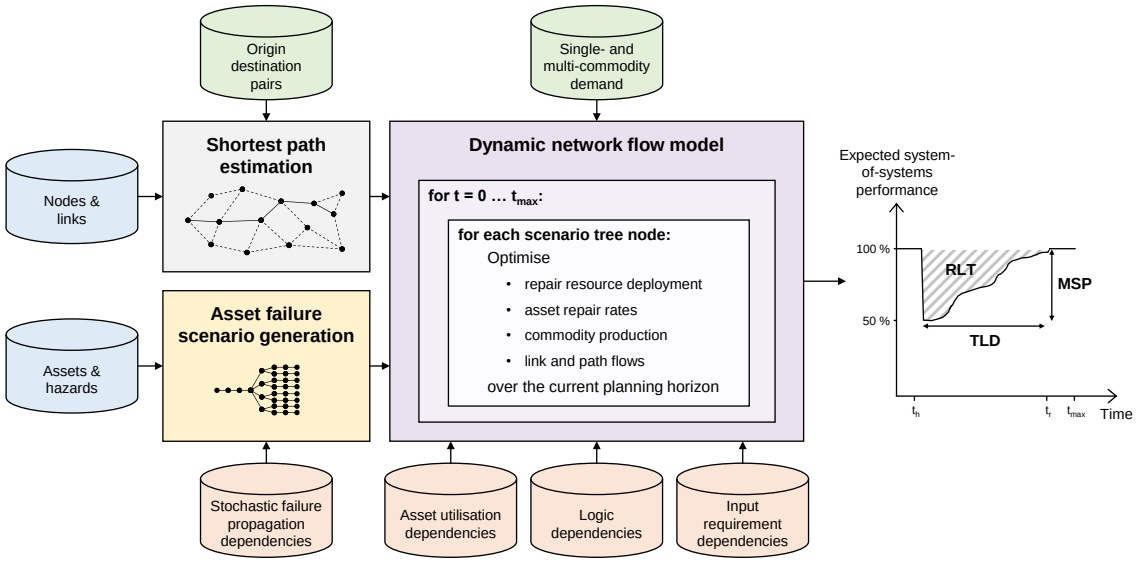

Figure 1 Overview of the modelling framework

3.1. Infrastructure systems

We represent infrastructure systems as networks (consisting of nodes and directed links) that are inter-connected with physical or non-physical assets. The network representation models the services provided by infrastructure systems. The asset representation models system components required for providing these services and their exposure to hazards.

Separating the network and asset representation enables us to extend the scope of the model with respect to network and asset effects independently of each other. Consider the example of a metro station. In the simplest case, it can be represented using one node and one asset. Network characteristics (i.e. the station's usage by passengers) could be modelled with greater detail by representing entrances, exits and platforms as separate nodes. Asset characteristics (i.e. the failure and repair of different components) could be modelled with greater detail by representing escalators, ventilation and lighting as separate sub-assets. There is no limit to increasing the level of detail by adding additional components to the asset and network mapping.

Assets can represent specific pieces of equipment (e.g. electricity transformers), buildings (e.g. metro stations or tunnels) or entire sub-systems (e.g. train control systems). Their operability is described by continuous variables $x_k^t \in [0,1]$. The occurrence of a hazard event or the propagation of

failure among interdependent assets can cause assets to fail, which would be represented by assigning the operability variables of affected components to $x_k^t = 0$. To regain their operability, assets require repair.

The network and asset representations of infrastructure systems are interdependent in the sense that network flows may require the utilisation of assets and the utilisation and repair of assets may require resources provided by networks. All inter- and intra-system dependencies are represented by directed dependency relations between nodes, links and assets.

3.2. Dependency relations

Several types of dependency relations have been identified in the literature. For example, Rinaldi et al. [9] define physical, cyber, geographic and logic dependencies. Zimmerman [11] distinguishes between functional and spatial dependencies. Dudenhoeffer et al. [12] describe physical, informational, geospatial, procedural and societal dependencies. A common characteristic of these typologies is their focus on the underlying cause of a dependency. This approach is useful for identifying and mapping dependencies. As far as modelling dependencies is concerned, we deem their effects as more important than their cause. Dependencies can have similar effects despite having different causes, or vice versa.

Consider, for example, the physical and cyber dependencies proposed by Rinaldi et al. [9], describing dependencies on material inputs from or information transmitted through another network. From a network flow modelling perspective, there is no fundamental difference between them, because in both cases a disruption of flows in the network supplying a service would disrupt flows in the dependent network.

In this paper, we propose a new, effect-based classification of dependency relations into four types: i) stochastic failure propagation, ii) logic, iii) asset utilisation, and iv) resource input dependencies. Figure 2 presents a simple example of two interdependent systems, which we will use in the following sub-sections to introduce how these dependencies are modelled.

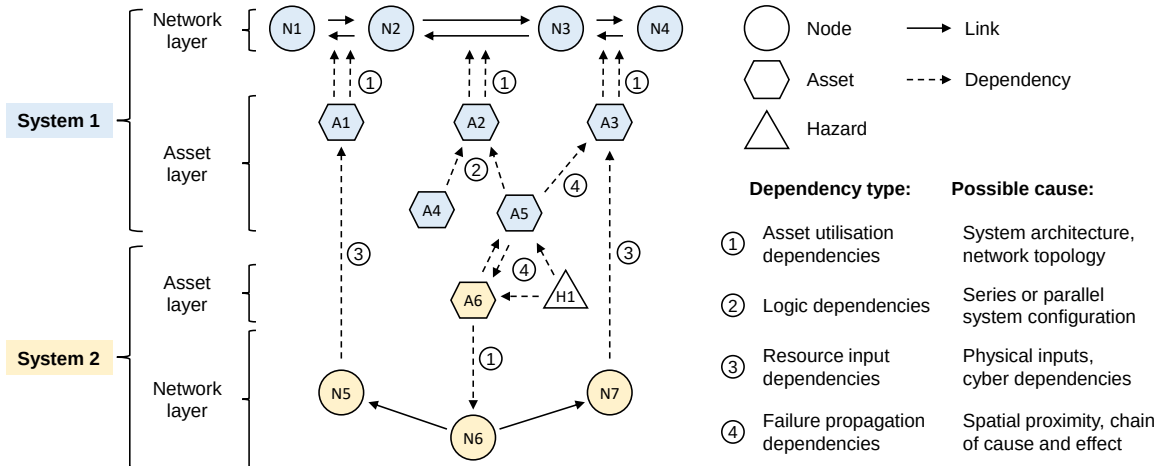

Figure 2 System representation and dependency types

3.2.1. Stochastic failure propagation dependencies

Failure propagation dependencies relate to geographic, spatial or co-location dependencies in cause-based typologies. They essentially describe a correlation between the failure probabilities of two assets, which could be the result of direct causation (e.g. the failure of a bridge damages railway tracks underneath it) or a shared hazard exposure (e.g. cables in a shared utility trench). Our modelling framework captuers failure propagation by considering an asset's failure probability a conditional probability depending on the occurance of hazard events and failure of other assets.

The example in Figure 2 contains five failure propagation dependencies, ultimately linked to a hazard H1 that affects assets A5 and A6. Due to spatial proximity, the failure of either one of these assets increases the probability that the other fails, which is represented by two directed failure propagation dependencies between them. If A5 fails, the failure can further propagate to A3.

Failure propagation dependencies are contained in the set D^{F} and specify the probability and time lag with which failures can propagate. For simplicity, we assume that there is no uncertainty regarding the time lag. Thus, each dependency relation $(k, m) \in D^{\mathrm{F}}$ is described by two parameters: the probability of failure propagation $p_{k,m}$ and time lag $t_{k,m}$.

For every failure propagation dependency and every time step of the simulation period, the model contains a binary random variable $Z_{k,m}^{t}$ that indicates whether the dependency is active ($Z_{k,m}^{t} = 1$) or not ($Z_{k,m}^{t} = 0$). These random variables are independent and Bernoulli distributed with $\Pr\left(Z_{k,m}^{t} = 1\right) = p_{k,m}$. If k is a hazard that is active at time t or an asset that fails at time t the failure spreads to the assets contained in the set $\left\{m\colon (k, m) \in D^{\mathrm{F}} \text{ and } Z_{k,m}^{t} = 1\right\}$.

Note that the model considers only one type of failure per asset. In cases where it is required to capture different failure modes, an asset is decomposed into sub-assets according to a fault tree analysis. Each sub-asset has its own failure mode and they are connected through logic dependencies.

3.2.2. Logic dependencies

We distinguish series system assets (contained in the sub-set A^{S}) and parallel system assets (contained in the sub-set A^{P}). For example, asset A2 in Figure 2 could represent a metro line modelled as a series system asset that requires the train control system (A4) and the railway track (A5) to be operational. The model could be extended by assuming that the train control system is a parallel system asset depending on two redundant control centres which would be added as sub-assets of A4.

The hierarchy of assets and sub-assets is captured by logic dependency relations contained in the set D^{L}. In contrast to failure propagation dependencies, we consider logic dependencies to be deterministic and have immediate effects. The operability of series system assets is constrained by the minimum operability of all assets that they depend on via a logic dependency relation:

$$\mathrm{x}_{\mathrm{k}}^{t} \leq x_{m}^{t} \qquad k \in A^{\mathrm{S}}, (m,k) \in D^{\mathrm{L}}, t = 0, \dots, t_{\max} \tag{6}$$

The operability of parallel system assets is constrained by the following equation:

$$x_{k}^{t} \leq \sum_{(m,k)\in D^{\mathrm{L}}} x_{m}^{t} \qquad k \in A^{\mathrm{P}}, t = 0, \dots, t_{\max} \tag{7}$$

This implies the assumption that the maximum operability of parallel system assets is a linear combination of the sub-systems' operabilities.

3.2.3. Asset utilisation dependencies

Asset utilisation dependencies are contained in the set D^{U} and connect the asset to the network representation in our modelling framework. Our toy model in Figure 2 contains seven asset utilisation dependencies, for example asset A1 is used by the two links (N1, N2) and (N2, N1), and asset A6 is used by the supply node N6.

We introduce asset utilisation variables $y_{k}^{t} \in [0,1]$ that are defined as the maximum capacity utilisation of all nodes and links depending on an asset. In the model, this is captured by inequality constraints

$$\frac{1}{\hat{f}_{i,j}} f_{\mathrm{i,j}}^{t} \leq y_{k}^{t} \qquad k \in A, \big(k, (i,j)\big) \in D^{\mathrm{U}}, t = 0, \dots, t_{\max} \tag{8}$$

$$\frac{1}{\hat{g}_{i}}\, g_{\mathrm{i}}^{t} \leq y_{k}^{t} \qquad k \in A, (k,i) \in D^{\mathrm{U}}, t = 0, \dots, t_{\max} \tag{9}$$

where $f_{\mathrm{i,j}}^{t}$ and g_{i}^{t} denote the current link flow and commodity generation at a dependent link or node respectively, and $\hat{f}_{i,j}$ and $\hat{g}_{i}$ denote the flow and generation capacities.

Asset utilisation dependencies have two effects. Firstly, if an asset fails and becomes inoperable the generation or transmission capacities of dependent nodes and links are reduced accordingly until the asset is repaired. This can be modelled by constraining the asset utilisation variable to be less than or equal to the asset operability variable:

$$y_{k}^{t} \leq x_{k}^{t} \qquad k \in A, t = 0, \dots, t_{\max} \tag{10}$$

The second effect of asset utilisation dependencies occurs in conjunction with resource input dependencies.

3.2.4. Resource input dependencies

Resource input dependencies contained in the set D^{I} also form a link between the two layers of the modelling framework, but in the opposite direction as asset utilisation dependencies. In the example in Figure 2, System 2 provides a resource to System 1, modelled by resource input dependencies (N5, A1) and (N7, A3).

The quantity of a resource input from node i to asset k is assumed to be proportional to the asset utilisation y_k^t with parameter $\alpha_{i,k}^{\mathrm{U}}$ and to the asset repair rate $\left(x_k^{t+1} - x_k^t\right)$ with parameter $\alpha_{i,k}^{\mathrm{R}}$. The total amount of resources supplied by i in time step t to all assets that depend on it can be calculated as follows:

$$\sum_{k \in A:(i,k) \in D^{\mathrm{I}}} \left(\alpha_{i,k}^{\mathrm{U}} y_k^t + \alpha_{i,k}^{\mathrm{R}}\left(x_k^{t+1} - x_k^t\right)\right) \tag{11}$$

In the case of supply shortages, resource input dependencies have the effect that the utilisation of an asset has to be reduced and / or its repair deferred until sufficient resources are available.

4. INTEGRATED ASSET OPERABILITY AND NETWORK FLOW MODEL

This section presents an integrated asset operability and network flow model that implements the modelling principles described above. Key elements of the methodology are a stochastic asset failure model, a scenario tree generation algorithm and a minimum cost flow assignment model.

4.1. Time-expanded asset-hazard graph

A hazard $h \in H$ in our model is assumed to occur at a specific time t_h. The uncertainty in the model stems from the stochastic failure propagation dependencies $(k, m) \in D^{\mathrm{F}}$, which can be active ($Z^t_{k,m} = 1$) or inactive ($Z^t_{k,m} = 0$). Given a sample of active failure propagation dependencies, we can create the time-expanded asset-hazard graph G^{AH}, whose node set is $A \cup H$ expanded over time steps $0, \dots, t_{\max}$. The link set contains the active failure propagation dependencies. Figure 3 depicts an asset-hazard graph for the example introduced in Figure 2. The graph visualises that in this specific sample the direct impact of the hazard event at $t_h = 1$ is the failure of asset A5 at $t = 2$. The second order impacts are the failures of A5 in the same time step and A3 at $t = 3$.

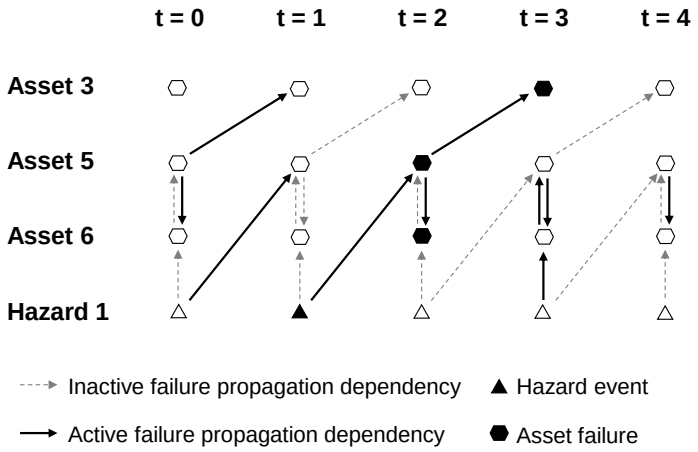

Figure 3 Time-expanded asset-hazard graph for the example in Figure 2

Let the variables z^t_k indicate whether an asset $k \in A$ fails ($z^t_k = 1$) or not ($z^t_k = 0$) at time t. Given a sample of failure propagation variables $\{Z^t_{k,m}, : (k, m) \in D^{\mathrm{F}}\}$ we can derive the asset failure variables $\{z^t_k : k \in A\}$ by constructing the asset-hazard graph and testing which nodes can be reached from an active hazard:

$$z^t_k = \begin{cases} 1 & \text{if } (k,t) \text{ can be reached from any } (h, t_h), h \in H \\ 0 & \text{otherwise} \end{cases} \qquad k \in A, t = 0, \dots, t_{\max} \tag{12}$$

Asset failures that are separated by only one failure propagation dependency from the hazard node are failures that occur as a direct impact of the hazard. Failures that are separated by more than one dependency can be considered as higher-order cascading failure effects.

4.2. Scenario tree generation

A simple way of integrating the stochastic asset failure model and flow assignment would be to create a number of asset failure samples and then carry out the network flow assignment for each scenario independently. Using such an approach, the flow assignment would have to be computed for $n_{\text{scn}} \times t_{\max}$ time steps, where n_{scn} denotes the number of scenarios. This would be computationally inefficient because the flow assignment computations would be redundant for the period before the first hazard event, in which all asset failure scenarios are identical.

A more efficient model integration approach is to generate a scenario tree, taking advantage of the fact that asset failure scenarios gradually diverge over time due to the uncertainty of failure propagation. Assuming that the first hazard occurs at t_h and the scenario tree immediately diverges from one to n_{scn} branches, the number of time steps for which the flow assignment has to be solved reduces to $t_h + n_{\text{scn}}(t_{\max} - t_h)$. In the average case, where divergence is slower, the number of necessary flow assignment computations is even lower.

The method used to generate a scenario tree is presented in Algorithm 1, which uses two parameters to control branching. Firstly, n_{spl} is the number of samples generated for each scenario tree node to populate the set of possible child nodes S_{children}. A higher value of n_{spl} would increase the rate of tree branching and capture a wider range of possible failure propagation. Moreover, it would increase the accuracy of the probability distribution over S_{children}, which is calculated as the number of times each sample value is observed divided by n_{spl}.

Tree branching is restricted by the second parameter n_{scn} in order to ensure that a maximum number of final scenarios is not exceeded and that the branching is distributed equally among all existing branches. The maximum number of child nodes added to the tree is

$$\left\lceil \frac{n_{\text{scn}} - |S_{t-1}|}{|S_{t-1}|} \right\rceil \tag{13}$$

where S_{t-1} is the set of scenario tree nodes in time step $t-1$. If the number of unique samples obtained from the stochastic asset failure model is greater than the value in (13), the required number of samples is selected randomly from the samples generated and the scenario probabilities are re-normalised.

Algorithm 1 Scenario tree generation

Algorithm ScenarioTreeGeneration

Input: Set of assets A, set of hazards H
Set of failure propagation dependencies D^{FP}
Maximum number of scenarios n_{scn}, Number of samples per parent node n_{spl}
Number of simulation time steps $t_{\max}$
Output: Scenario tree S
Initialise $S_t = \{\}$ for $t = 0, \dots, t_{\max}$
New scenario tree node s_{root}
Probability(s_{root}) ← 1
AssetFailure(s_{root}) ← $\{z_k^0 = 0, k \in A\}$
Add s_{root} to S_0
For $t = 1, \dots, t_{\max}$
  For each s_{parent} in S_{t-1}
    $S_{\mathrm{children}} = \{\}$
    For $i = 1, \dots, n_{\mathrm{spl}}$
      New scenario tree node s_{sample}
      Parent(s_{sample}) ← s_{parent}
      Probability(s_{sample}) ← Probability(s_{parent}) / n_{spl}
      Sample failure propagation variables $Z_{k,m}^t$ and create asset hazard graph
      AssetFailure(s_{sample}) ← $\left\{ z_k^t = \begin{cases} 1 & \text{if } (k,t) \text{ is reachable from any } (h,t_h), h \in H \\ 0 & \text{otherwise} \end{cases}, k \in A \right\}$
      If S_t contains any s_{ident} where AssetFailure(s_{ident}) == AssetFailure(s_{sample})
        Probability(s_{ident}) ← Probability(s_{ident}) + Probability(s_{sample})
      Else
        Add s_{sample} to S_{children}
    If $|S_{\mathrm{children}}| > \left\lceil \frac{n_{\mathrm{scn}} - |S_{t-1}|}{|S_{t-1}|} \right\rceil$
      Randomly discard $|S_{\mathrm{children}}| - \left\lceil \frac{n_{\mathrm{scn}} - |S_{t-1}|}{|S_{t-1}|} \right\rceil$ child nodes from S_{children}
      Normalise probabilities in S_{children}
    Add S_{children} to S_t
Return $S = [S_0, S_1, \dots, S_T]$

4.3. Dynamic network flow model

The dynamic network flow model used in this paper is based on a minimum cost flow assignment method, deployed in a rolling planning horizon framework and extended with three types of dependency relations (asset utilisation, resource input, logic) and the optimisation of asset repair.

4.3.1. Rolling planning horizon

Holden et al. [20] model dynamic flows by solving a separate minimum cost flow problem for each time step. However, this technique cannot model flows with a duration greater than the length of one time step and does not allow foresight and planning. The latter point is particularly relevant for models with repairable systems and limited repair capacity because optimal repair strategies have to anticipate where network capacity is most needed in order to prioritise repair. These limitations can be overcome by transforming the network into a time-expanded network [52]. However, with this technique the size of the resulting optimisation problem increases linearly with the number of time steps, limiting the

scalability of the method. Moreover, the transformation into a single optimisation problem for all time steps means that the model assumes perfect foresight, which is arguably as unrealistic as the assumption of no foresight. While it is realistic that system operators anticipate the results of their own actions, such as repair measures, it is unrealistic that they can fully anticipate random events, such as equipment failure.

The model presented in this paper combines the iterative and time-expanded network approaches by using a rolling planning horizon with a length of t_{ph} time steps. Iterating the current time step t_{c} through the simulation period $0, \dots, t_{\max}$, a time-expanded network flow problem is solved for each planning horizon $t_{\mathrm{c}}, \dots, t_{\mathrm{c}} + t_{\mathrm{ph}}$. However, only the optimal values of the decision variables for the first time step of each planning horizon are saved as simulation results. The flows computed for time steps $t_{\mathrm{c}} + 1, \dots, t_{\mathrm{c}} + t_{\mathrm{ph}}$ indicate what is anticipated at time t_{c}. These predictions are updated in subsequent iterations and the final value of a decision variable is obtained when its respective time step becomes the current time step.

Combining the iterative and time-expanded network approaches has two important advantages. Firstly, it limits the size of the optimisation problems to t_{ph}-times the size of the corresponding static network flow problem. Secondly, it provides a higher degree of realism than both approaches by themselves. The consequences of decisions, for example regarding routing and repair, can be anticipated, but not random events, such as asset failure. The model reflects how the planning is revised after each time step as new information becomes available.

4.3.2. Linear programming formulation

The minimum cost flow assignment method can be formulated as a linear programming (LP) optimisation problem [53]. The method requires the k shortest paths for each OD pair, which can be obtained in a pre-processing step using Yen's algorithm [54].

The LP decision variables are non-negative and indexed with superscript $t = t_{\mathrm{c}}, \dots t_{\mathrm{c}} + t_{\mathrm{ph}}$ for the time steps in the current planning horizon. They comprise link flow variables $f_{i,j}^{t}$ for links $(i,j) \in E$, path flow variables f_{p}^{t} for paths $p \in P_{o,d}$ between OD pairs $(o,d) \in OD$, as well as commodity generation variables g_{i}^{t} and commodity utilisation variables u_{i}^{t} for single-commodity nodes $i \in E^{\mathrm{SC}}$. In addition to these conventional decision variables for network flow models, we include the decision variables x_{k}^{t} and y_{k}^{t} for the operability and utilisation of infrastructure assets $k \in A$ to enable the modelling of dependencies between the asset and network representations as well as optimisation of asset repair. The complete LP formulation of the model is as follows:

$$\min \sum_{t=t_c}^{t_c+t_{ph}} \left(\sum_{(i,j)\in E} c_{i,j}^{f} f_{i,j}^{t} + \sum_{i\in V^{SC}} c_i^{g} g_i^{t} + \sum_{i\in V^{SC}} v_i^{SC}(\breve{u}_i^{t} - u_i^{t}) + \sum_{(o,d)\in OD} v_{o,d}^{MC} \left(\breve{f}_{o,d}^{t} - \sum_{p\in P_{o,d}} f_p^{t} \right) \right) \tag{14}$$

s.t.

$$f_{i,j}^{t}, f_p^{t}, g_i^{t}, u_i^{t}, x_k^{t}, y_k^{t} \geq 0 \qquad \begin{matrix}(i,j)\in E, p\in Q_{i,j},\\ i\in V^{SC}, k\in A,\\ t=t_c,\dots,t_c+t_{ph}\end{matrix} \tag{15}$$

$$u_i^{t} \leq \breve{u}_i^{t} \qquad i\in V^{SC}, t=t_c,\dots,t_c+t_{ph} \tag{16}$$

$$\sum_{p\in P_{o,d}} f_p^{t} \leq \breve{f}_{o,d}^{t} \qquad (o,d)\in OD, t=t_c,\dots,t_c+t_{ph} \tag{17}$$

$$f_{i,j}^{t} = \sum_{p\in Q_{i,j}} f_p^{t-\delta(p,i)} \qquad (i,j)\in E^{MC}, t=t_c,\dots,t_c+t_{ph} \tag{18}$$

$$x_k^{t} \leq 1 \qquad k\in A, t=t_c,\dots,t_c+t_{ph} \tag{19}$$

$$x_k^{t_c} \leq \begin{cases} 0 & \text{if } z_k^{t_c}=1 \\ \bar{x}_k^{t_c} & \text{otherwise} \end{cases} \qquad k\in A \tag{20}$$

$$x_k^{t-1} \leq x_k^{t} \qquad k\in A, t=t_c+1,\dots,t_c+t_{ph} \tag{21}$$

$$x_k^{t} \leq x_m^{t} \qquad \begin{matrix}k\in A^{S}, (m,k)\in D^{L},\\ t=t_c,\dots,t_c+t_{ph}\end{matrix} \tag{22}$$

$$x_k^{t} \leq \sum_{(m,k)\in D^{L}} x_m^{t} \qquad k\in A^{P}, t=t_c,\dots,t_c+t_{ph} \tag{23}$$

$$f_{i,j}^{t} \leq \hat{f}_{i,j} \qquad (i,j)\in E, t=t_c,\dots,t_c+t_{ph} \tag{24}$$

$$g_i^{t} \leq \hat{g}_i \qquad i\in V^{SC}, t=t_c,\dots,t_c+t_{ph} \tag{25}$$

$$\frac{1}{\hat{f}_{i,j}} f_{i,j}^{t} \leq y_k^{t} \qquad \begin{matrix}k\in A, (k,(i,j))\in D^{U},\\ t=t_c,\dots,t_c+t_{ph}\end{matrix} \tag{26}$$

$$\frac{1}{\hat{g}_i} g_i^{t} \leq y_k^{t} \qquad \begin{matrix}k\in A, (k,i)\in D^{U},\\ t=t_c,\dots,t_c+t_{ph}\end{matrix} \tag{27}$$

$$y_k^{t} \leq x_k^{t} \qquad k\in A, t=t_c,\dots,t_c+t_{ph} \tag{28}$$

$$g_i^{t} - u_i^{t} - \sum_{k\in A:(i,k)\in D^{I}} \left(\alpha_{i,k}^{U} y_k^{t} + \alpha_{i,k}^{R} \left(x_k^{t+1} - x_k^{t} \right) \right) + \sum_{j\in V:(j,i)\in E} f_{j,i}^{t-\tau(j,i)} - \sum_{j\in V:(i,j)\in E} f_{i,j}^{t} = 0 \qquad i\in V^{SC}, t=t_c,\dots,t_c+t_{ph} \tag{29}$$

The objective (14) comprises the cost of link flows and commodity generation, and penalty terms for unmet demand in single- and multi-commodity networks, summed over all time steps in the current planning horizon.

Constraints (16) and (17) ensure that the supply of infrastructure services cannot exceed the demand given by parameters $\breve{u}_i^t$ and $\breve{f}_{o,d}^t$ for single- and multi-commodity networks respectively.

Constraints (18) ensure consistency between link and path flows in multi-commodity networks. The notation $Q_{i,j}$ is used for the set of all paths that make use of a link $(i,j) \in E^{\mathrm{MC}}$. Flows can stretch over more than one time step and the time step index of flow variables indicates the departure time. We use the path transit time function $\delta(p,i)$ to express how many time steps after the departure from its origin a flow on path p leaves the intermediate node i.

Asset operability variables x_k^t are constrained to values between 0 and 1 as per (19). If the current asset failure scenario includes the failure of an asset $k \in A$ at time t_{c} the binary variable $z_k^{t_{\mathrm{c}}}$ has the value one and equation (20) sets the initial operability $x_k^{t_c}$ equal to zero. Otherwise, the initial operability is set to $\bar{x}_k^t$, which denotes the operability after the optimal repair action identified in the previous iteration has been carried out.

Constraints (21) enforce that the operability variables cannot decrease over the planning horizon. This means that the optimisation only considers asset failures which have already occurred at the current time step and does not anticipate additional failure events within the planning horizon. Nevertheless, such failures can take place in the stochastic simulation and will then affect subsequent iterations of the dynamic network flow model. Constraints (22) and (23) implement logic dependency relations as described in Section 3.2.2.

Constraints (24) and (25) set the nominal capacity for link flows and commodity generation. Constraints (26) and (27) relate capacity utilisation and asset utilisation according to the concept of asset utilisation dependencies introduced in Section 3.2.3. Constraints (28) set the operability of an asset as the upper limit for its utilisation.

Finally, conservation of flow constraints are formulated in (29). They ensure a balance at each node between commodity generation, commodity utilisation, commodity supply for the utilisation and repair of dependent assets (as described in Section 3.2.4), and the net flow over connected links. The link transit time function $\tau(j,i)\colon E \to \mathbb{N}$ is used to define how many time steps after the departure at node j a flow arrives at node i.

The size of the LP formulated in Equations (14) to (29) is considerable for city-scale infrastructure networks with hundreds or thousands of nodes, links, OD pairs and assets. The number of decision variables is $t_{\mathrm{ph}}\left(2\left|V^{\mathrm{SC}}\right| + |E| + k|OD| + 2|A|\right)$ and an upper bound for the number of constraints is $t_{\mathrm{ph}}\left(3\left|V^{\mathrm{SC}}\right| + |OD| + 2|E| + 3|A| + \left|D^{\mathrm{L}}\right| + \left|D^{\mathrm{U}}\right|\right)$. Owing to the computational efficiency of the simplex algorithm, solutions to LP problem instances of this magnitude can be obtained within seconds or minutes, thus enabling the analysis of a large scenario tree.

4.4. Simulation experiments

The process for conducting a simulation experiment with the integrated asset operability and dynamic network flow model is described in Figure 4. After the dynamic network flow problem is solved, the remaining legs of journeys that could not be completed in the first time step of the planning horizon are added as an additional demand to all scenarios derived the respective scenario tree node. If such continued journeys are not between an existing OD pair, Yen's algorithm is used again to find the k shortest paths.

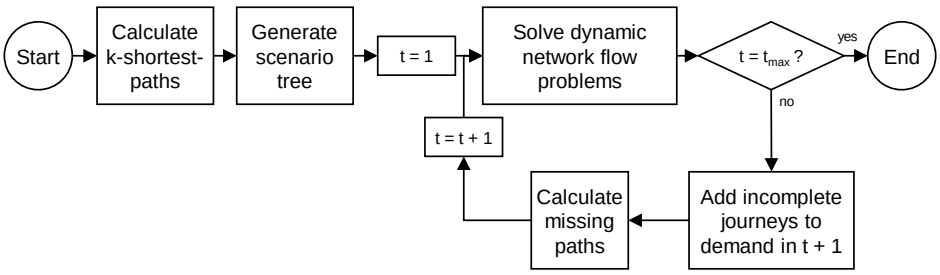

Figure 4 Flow chart of the integrated asset failure and network flow simulation

A bespoke modelling and simulation environment was developed using the C# language to implement the combined stochastic asset failure and dynamic network flow model. Several parts of the modelling methodology lend themselves for parallel processing, namely shortest path finding, scenario tree expansion and flow assignment for different scenarios within the same time step.

5. CASE STUDY OF CRITICAL INFRASTRUCTURE IN LONDON

To demonstrate and test the resilience assessment methodology proposed in this paper, we present a case study of critical infrastructure systems in London. The case study aims to quantify the resilience of the electricity distribution and metro networks against a hypothetical flood hazard, taking into account various interdependencies between the two systems.

5.1. Data sources and modelling assumptions

The case study uses real-world data from several different sources and also makes a number of modelling and parameter assumptions where data were unavailable, mostly regarding the risk exposure and repair of infrastructure assets. Table 4 in the appendix provides an overview of the parameters used to capture the structure and behaviour infrastructure systems. The parameters of dependency relations are presented in Table 5. Both tables make references to Table 6 which summarises the key assumptions of this case study.

5.1.1. Infrastructure systems

The model contains four infrastructure systems: the London Power Network (LPN), London Underground Network (LUN), and two repair resource networks that provide repair services to assets in the LPN and LUN respectively.

The LPN is an electricity distribution network owned and operated by UK Power Networks who provide detailed network data in the context of their long term development statement (LTDS) [55]. The system consists of more than 35,000 kilometres of cable, serves around 2.3 million customers, and delivers 4.8 GW during peak demand. The 1,379 nodes of the network include 67 super-grid transformers, where power is fed into the systems, and 128 demand nodes, most of which represent substations at the 11 kV level. The LPN contains 1,742 links representing connectors and transformers, and 392 assets representing substations.

The main data source for the LUN is Transport for London's Rolling Origin and Destination Survey (RODS) [56]. This dataset is produced based on passenger surveys to capture information on journeys on the London Underground on a typical weekday. The daily travel demand consists of 4.8 million passenger journeys between 32,109 OD pairs. There are 1,045 nodes in the LUN, representing stations and their platforms, and 2,315 links. The asset layer consists of 389 assets, including metro stations, track sections, line control systems, control centres, rolling stock fleets and depots.

Due to the unavailability of data on specific repair resources and processes for the two infrastructure systems, the LPN and LUN repair systems are modelled as radial, single-commodity networks that connect engineering depots with potential repair sites associated to individual physical assets. Flows in the repair systems are abstract representations of the repair services that engineering depots provide to

assets. The model assumes that the complete repair of any asset (from $x_k^{t_1} = 0$ to $x_k^{t_2} = 1$) requires one unit of this repair service.

5.1.2. Hazard

To demonstrate how the model can be used to carry out a resilience assessment, a hypothetical flooding incident is assumed as an example hazard. The borough of Brent was chosen as the case study area because several infrastructure assets in this area are located close to a potential source of flooding, the Welsh Harp reservoir. The borough's strategic flood risk assessment [57] and flood risk management strategy [58] identify a failure of this reservoir as the most catastrophic, yet unlikely flooding incident. The reports do not quantify the probability of such an incident, but they state that the failure probability for similar reservoirs is estimated to be one in 50,000 years. This is substantially lower than the probability of flooding scenarios considered in current flood protection policies. Nevertheless, it was deemed a suitable example for this case study because it demonstrates how the proposed method is particularly apt for exploratory analysis of high-impact, low-probability events.

It is not in the scope of this paper to carry out detailed flood risk assessments for individual assets. Instead, we assume that the risk of flood damage depends only on whether an asset is located in one of the two flood zones shown in Figure 5. Flood zone 1 extends 2,000 m downstream of the reservoir and contains 9 infrastructure assets. Flood zone 2 encompasses the area between 2,000 and 4,000 m downstream of the reservoir and contains 30 assets.

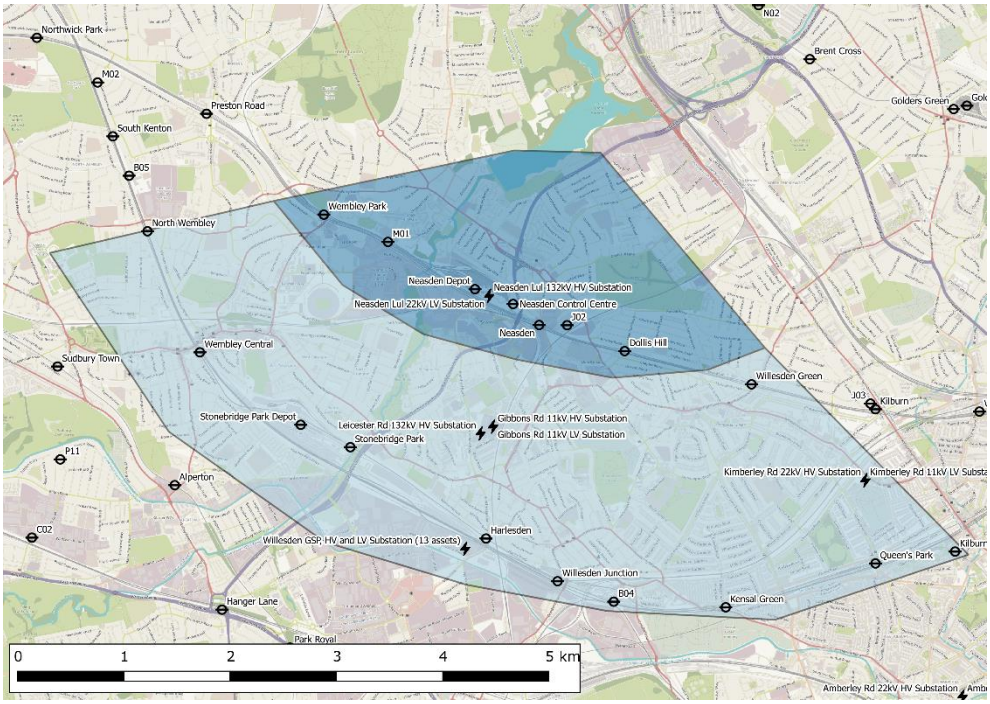

Figure 5 Infrastructure assets in the two impact zones of the hypothetical flooding incident

5.1.3. Dependency relations

Dependencies relations are added to the model following the 14 rules presented in Table 5 (see appendix). The asset utilisation and logic dependencies are directly deduced from the system architecture. Input dependencies model the supply of electricity to operate metro stations and trains. Furthermore, each asset is connected to its repair site node via an input dependency. Failure propagation dependencies are added based on the geographic distance of an asset to the hazard or to another asset (assumptions A 10 and A 11). In total, the model contains 16,295 dependency relations.

5.1.4. Model validation

The LUN flow assignment was validated for the no disruption case by comparing the predicted passenger flows between adjacent stations to the estimated line loading provided in the RODS dataset. The mean absolute percentage error for the morning peak hour is 14.1 %. Line loading data for the LPN was not available and the flow assignment was only validated by checking that the demand at all substations is fully satisfied in the no disruption case.

Errors regarding the predicted network flows are to be expected considering the use of a minimum cost flow method that models neither passengers' route choice behaviour beyond shortest-path seeking nor physical laws governing power flows. However, the accuracy of the minimum cost flow method is deemed sufficient for the purpose of this case study and for initial resilience assessments in general. The envisioned workflow for a comprehensive resilience assessment with the proposed modelling framework is that, in the first instance, a large number of scenarios is analysed using the computationally efficient minimum cost flow method. In a second step, a smaller number of representative scenarios can be analysed with more computationally demanding and infrastructure-specific assignment models.

Asset failures and repairs simulated in this case study are verified against the modelling assumptions but not validated using real-world data because parameters for hazard exposure and repair capabilities are hypothetical. Resilience assessment models for extreme events are generally difficult to validate due to the unavailability of historical data. When used in practice, the model proposed in this paper should be validated with the help of subject matter experts who can check individual model inputs, such as failure probabilities and repair capacities.

5.2. Simulation

We conduct a simulation experiment assuming that the flooding incident takes place at 8 a.m. on a weekday. The simulation parameters are given in Table 3.

Table 3 Simulation parameters

Parameter	Description	Value
$t_{\max}$	Length of simulation period	24 hours
t_{ph}	Length of planning horizon	5 hours
n_{scn}	Max. no. of scenarios	150
n_{spl}	No. of samples per scenario tree node	10
k	No. of shortest paths	10

Using the algorithm presented in Section 4.2, we generated a scenario tree with 74 unique asset failure scenarios. The LP problem instances had an average of 230,000 decision variables, 100,000 constraints and 4 million non-zero constraint matrix coefficients. They were solved using the Gurobi dual simplex solver version 8.0.0. On a 3.50 GHz CPU the average runtime was 30 seconds per LP problem instance. The model lends itself to parallel computing, as the calculations for each branch in the scenario tree are independent of each other. On a CPU with six cores, it took approximately one hour to pre-calculate the shortest paths and 3 hours to run the simulation.

5.3. Results

The simulation experiment provides insights into how the flooding incident could affect the performance of the two infrastructure systems, given our simplifying assumptions on failure propagation and repair processes.

5.3.1. Asset failure and repair

Asset inoperability caused by direct and propagated failure after the flooding incident is shown in Figure 6. In the first hour after the incident ($t = 8$), the expected number of asset failures over all scenarios is 1.4 and 0.5 in the LUN and LPN respectively. In the second hour after the incident, the total inoperability in the LUN system is expected to decrease to 1.1 due to the effective deployment of repair resources which outweighs the additional damage caused by direct damage in flood zone 2 (0.2) and failure propagation (0.2). In contrast, the total inoperability in the LPN system is predicted to rise sharply to 8.0, mainly due to failure propagation (6.8) and also to direct damage in the second flood zone (0.9). Due to the large number of asset failures, the LPN system is predicted to take 10 hours until full recovery of asset operability whereas the LUN network is predicted to take only 5 hours.

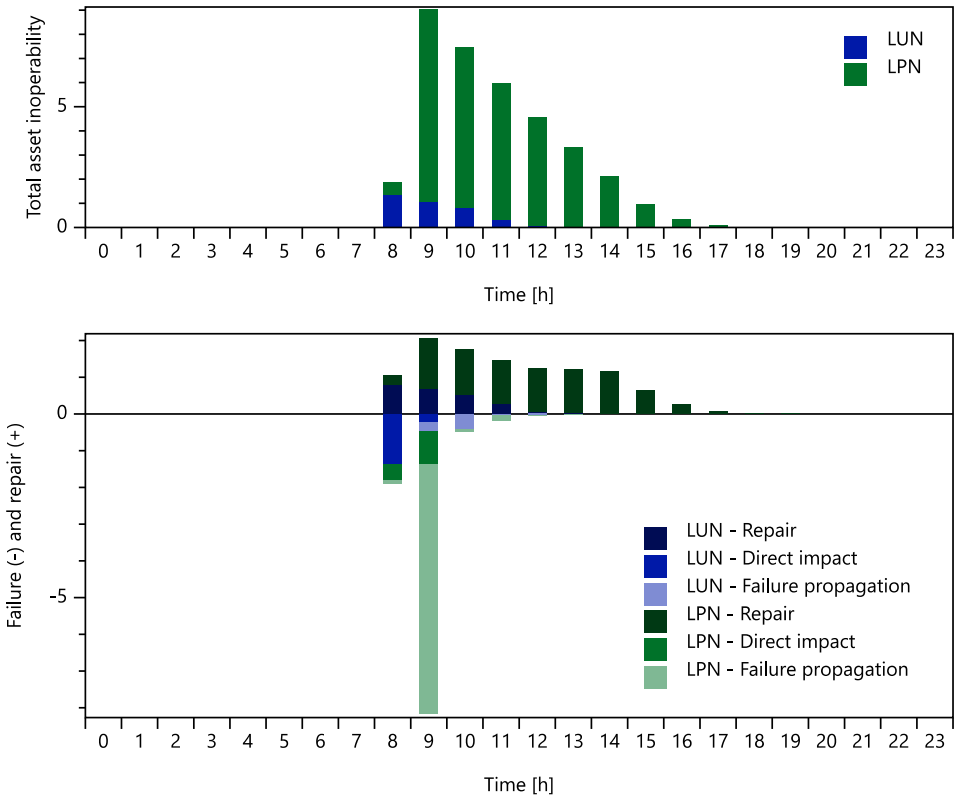

Figure 6 Total asset inoperability (top) and changes in asset operability (bottom)

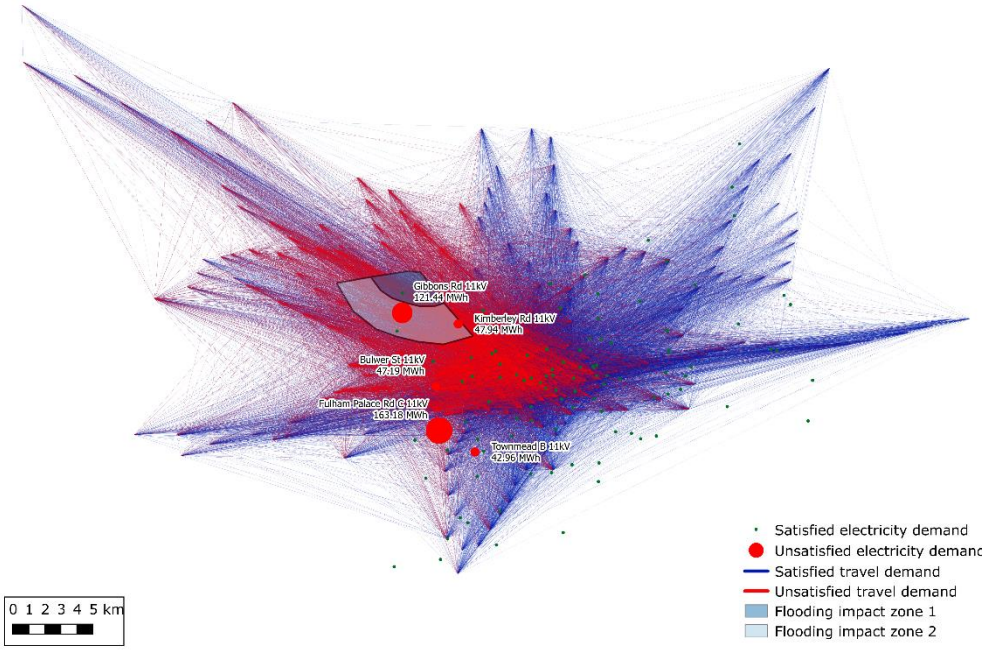

Figure 7 Electricity demand nodes and origin-destination pairs affected by the flooding incident

5.3.2. *Unmet demand*

The asset inoperability predicted by the model would severely affect the systems' ability to meet the demand of a typical weekday. Although the flood damage is contained to a relatively small area of the city, its effects spread widely, as shown on the map of unmet demand in Figure 7.

The expected loss of electric power supply to two demand nodes located within the second flood zone amounts to 172 MWh over the duration of the disruption. Additional 253 MWh of unmet demand are expected to occur at three substations which are located south of the area affected by flooding.

The disruptions in the metro network mainly affect the Jubilee, Metropolitan and Bakerloo lines, which run through the area affected by flooding and also depend on rolling stock, train control and electric power supply assets located there. Hence, most journeys that are cancelled or delayed are to or from areas served by these lines, most notably the Northwest of London. In total, the model predicts that journeys between 7,321 OD pairs with a combined travel volume of 66,166 passenger journeys would be affected by the disruption.

5.3.3. *Value of demand and supply*

The model predicts the expected loss (the difference between the value of demanded and supplied infrastructure services) to amount to 1.3 and 7.2 million GBP in the transport and energy sectors respectively. These results depend strongly on our assumptions regarding the value of infrastructure services (A 2 and A 9). Figure 8 shows that although the estimated loss is in the range of millions, it is still relatively small compared to the overall value of services provided by the infrastructure networks.

The simulation experiment enables us to quantify the resilience of the two interdependent infrastructure systems in terms of the resilience measures introduced in Section 2. Figure 9 plots the value-based system performance $\left(1 - \frac{\mathrm{VoS}_t}{\mathrm{VoD}_t}\right)$ for the 74 individual scenarios and its probability-weighted average over all scenarios. The model predicts an average resilience loss triangle area (RLT) of 0.11, an expected minimum system performance of 0.96 and a total length of disruption of 9 hours.

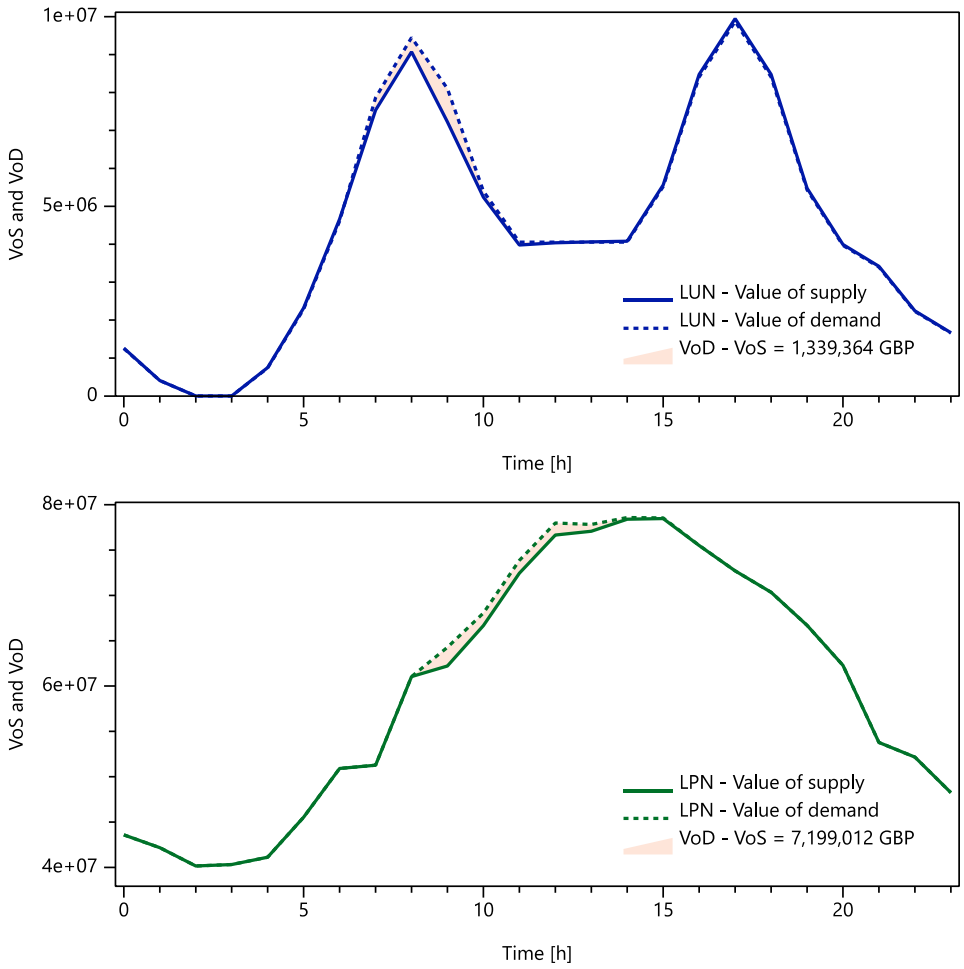

Figure 8 Value of demand (VoD) and expected value of supply (VoS)

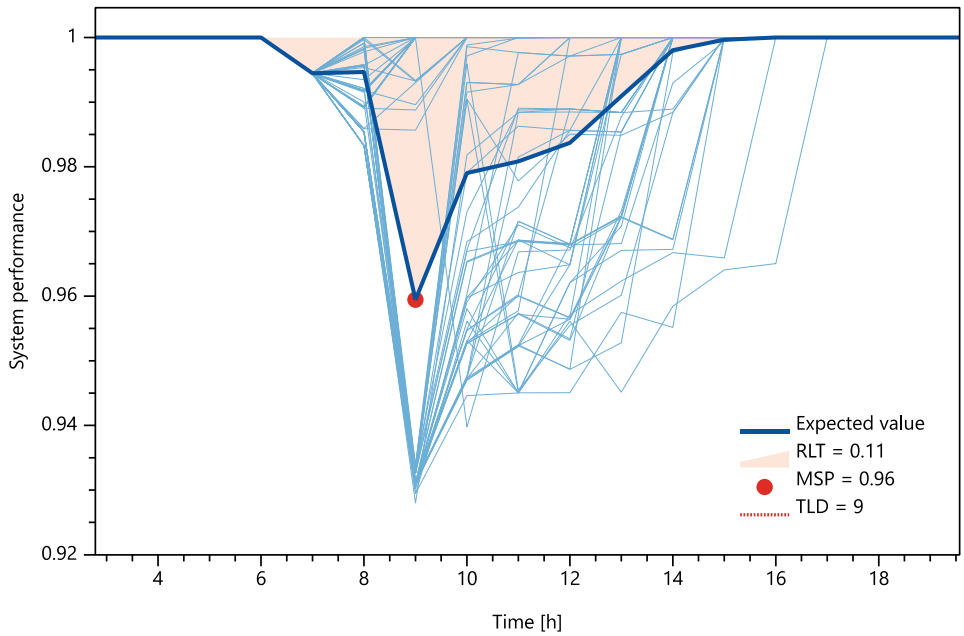

Figure 9 Value-based system performance index

5.4. Sensitivity analysis

The simulation experiment was repeated with different parameter settings to analyse sensitivity. The parameter for the capacity of engineering depots providing repair services was varied over the set $\{0, 1, 2, 3\}$. Furthermore, three different levels for failure propagation probabilities were assumed. In the first setting, the probability for short-range failure propagation (from the hazard to assets in flood zone 1 or between assets less than 100 m apart) is 0.125 and the probability for long-range failure propagation (from the hazard to assets in flood zone 2 or between assets 100 to 1,000 m apart) is 0.025. In the second setting, the probabilities are 0.250 and 0.050 respectively, and in the third setting they are 0.500 and 0.100. The predicted RLT values for the resulting 12 parameter configurations are presented in Figure 10. As expected, the sensitivity analysis shows that increasing the probability of failure propagation increases the RLT area whereas increasing the capacity to provide repair services decreases it.

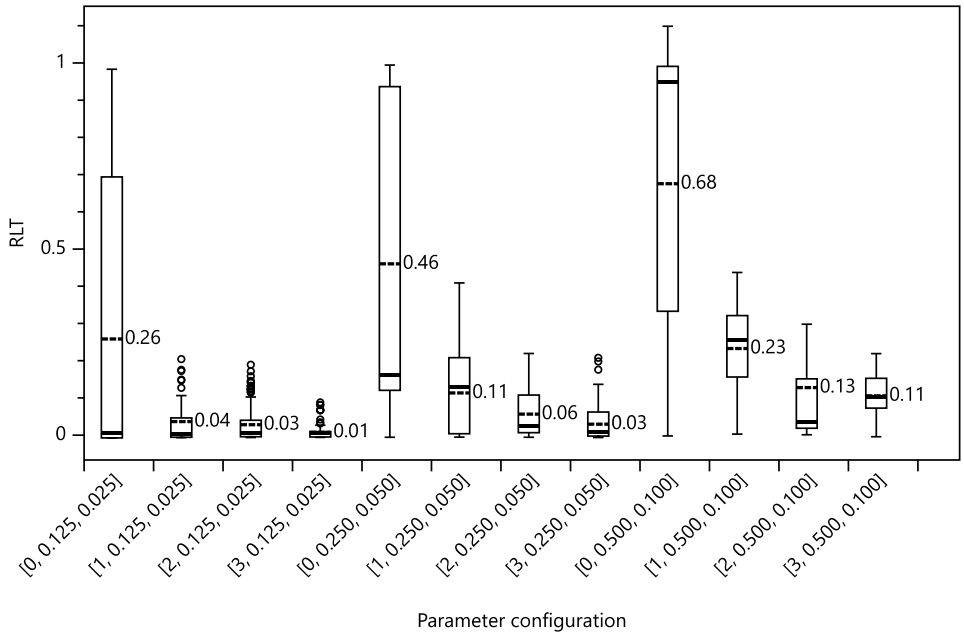

Figure 10 RLT area for 12 parameter configurations denoted by [repair capacity, probability of short-range failure propagation, probability of long-range failure propagation]. Dashed lines indicate the probability-weighted mean.

The sensitivity analysis also demonstrates how the modelling framework presented in this paper could be used to inform decision-making on how to improve the resilience of interdependent infrastructure systems. For example, assume that the status quo is best represented by the parameter setting [1, 0.250, 0.050] with an RLT area of 0.11. The model suggests that the resilience could be improved to 0.06 at the cost of doubling the resources available for asset repair. Alternatively, the resilience could be improved to 0.04 by investing in the protection of assets so that they are 50 % less likely to suffer flood damage. A cost-benefit analysis based on such modelling and simulation results

could help decision-makers optimise strategies for strengthening infrastructure resilience and save considerable financial resources compared to interventions not based on such evidence.

5.5. Discussion

The case study shows that the methodology presented in this paper can be used to create a complete model of two real-world urban infrastructure networks relying only on publicly available data. Some assumptions had to be made where data were not available, for example regarding hazard exposure and repair resources. However, it is expected that future users of this modelling framework (e.g. infrastructure companies) would be able to replace most of the assumptions with empirical data, thereby improving the validity and accuracy of the analysis.

The case study illustrates that combining the network and asset representations of infrastructure systems increases the level of detail at which infrastructure systems and their interdependencies can be modelled. Aspects of infrastructure operations captured by this methodology that are outside the scope of many existing models include the stochastic propagation of asset failure, hierarchical relations of series or parallel sub-systems, and resource inputs from one system to another for the utilisation and repair of assets.

Using a time-expanded graph and a rolling planning horizon, the method presented in this paper models the optimal response to a disruption in terms of flow redistribution and repair resource allocation. The model is based on the assumption that stochastic asset failure cannot be anticipated but the effects of deploying repair resources can. However, the modelling framework would allow to modify these assumptions. For example, one could include anticipation of asset failure based on (limited) knowledge of failure propagation dependencies or a stochastic variation of repair effectiveness.

Even with the high level of operational detail captured by the proposed methodology, a dynamic, city-scale model of two infrastructure systems with several thousands of assets, nodes, links and dependency relations can be modelled and simulated with the computational resources of a standard desktop computer. Compared to case studies presented for previous network flow models for interdependent infrastructure networks, the system-of-systems analysed here is considerably larger and the results offer more detailed insights into the phenomena determining infrastructure performance after disruptive events.

While the minimum cost flow assignment model does not achieve the accuracy of more sophisticated infrastructure-specific assignment models, it is suitable for resilience assessments seeking to cover a large number of possible disruption scenarios. Its role in the modelling framework can be seen as a placeholder model that can be replaced with more accurate assignment models if the required data inputs for the latter are available and a smaller number of representative scenarios has been identified.

The optimisation problem formulated in this paper can be solved efficiently even for large problem instances because it makes several approximations to avoid integer variables and non-linear equations.

For instance, the operability of a parallel system is assumed to be a linear combination and not the maximum of the sub-systems' operabilities. Resource inputs required by an asset are proportional to the asset's utilisation and do not include inputs that are required simply for the availability of an asset (e.g. a metro station's electric power base load). Such non-linear relationships could be modelled by introducing binary decision variables but this would drastically increase the computational complexity.

6. CONCLUSION

By combining the network flow modelling paradigm with a novel representation of repairable infrastructure assets, this paper makes some important contributions to improving resilience assessment methods for interdependent infrastructure systems. An integrated and dynamic modelling framework is presented that features a scenario tree generation algorithm for stochastic failure propagation and the optimisation of network flows and repair resource allocation in response to a disruption. A rolling planning horizon approach allows the model to make realistic assumptions regarding the anticipation of asset failure and repair and enables the analysis of infrastructure resilience as opposed to static network vulnerability.

The proposed modelling framework can be used by asset owners, network operators and infrastructure planners to quantify the effects of changes regarding the configuration of infrastructure systems and their exposure to hazards. Examples of interventions that could be evaluated include investments in additional protection for infrastructure assets or resources for incident response. Users of the model could either predict how the resilience performance measures would change after the interventions or conduct experiments to estimate the investments required to achieve a certain level of resilience against anticipated future hazard scenarios. The use of a value-based resilience measure allows the direct use of model outputs in a cost-benefit analysis.

Further research could investigate in more detail how the linearity assumptions of the minimum cost flow model affect the results and how the use of binary switching variables would affect its computational complexity. Another direction of research could be to use the model presented here to develop a criticality ranking method for infrastructure assets in a system-of-systems. Finally, it is anticipated that future studies will extend the model to other types of infrastructure networks, for example, road transport and communication networks.

7. ACKNOWLEDGEMENTS

The research was supported by the UK Engineering and Physical Sciences Research Council (EPSRC) as part of the Sustainable Civil Engineering Centre for Doctoral Training (grant number EP/L016826/1).

REFERENCES

[1] M. Kunz, B. Mühr, T. Kunz-Plapp, J. E. Daniell, B. Khazai, F. Wenzel, M. Vannieuwenhuyse, T. Comes, F. Elmer, K. Schröter, J. Fohringer, T. Münzberg, C. Lucas, and J. Zschau, "Investigation of superstorm Sandy 2012 in a multi-disciplinary approach," *Nat. Hazards Earth Syst. Sci.*, vol. 13, no. 10, pp. 2579–2598, 2013.

[2] S. Kaufman, C. Qing, N. Levenson, and M. Hanson, "Transportation During and After Hurricane Sandy," 2012. [Online]. Available: http://wagner.nyu.edu/files/rudincenter/sandytransportation.pdf. [Accessed: 04-May-2018].

[3] The City of New York, "A Stronger, More Resilient New York," 2013. [Online]. Available: http://www.nyc.gov/html/sirr/html/report/report.shtml. [Accessed: 11-May-2017].

[4] S. E. Chang, T. L. McDaniels, J. Mikawoz, and K. Peterson, "Infrastructure failure interdependencies in extreme events: power outage consequences in the 1998 Ice Storm," *Nat. Hazards*, vol. 41, pp. 337–358, Nov. 2007.

[5] M. Rong, C. Han, and L. Liu, "Critical Infrastructure Failure Interdependencies in the 2008 Chinese Winter Storms," in *2010 International Conference on Management and Service Science (MASS)*, 2010.

[6] L. Dueñas-Osorio and A. Kwasinski, "Quantification of Lifeline System Interdependencies after the 27 February 2010 Mw 8.8 Offshore Maule, Chile, Earthquake," *Earthq. Spectra*, vol. 28, no. S1, pp. S581–S603, Jun. 2012.

[7] T. D. O'Rourke, S.-S. Jeon, S. Toprak, M. Cubrinovski, M. Hughes, S. van Ballegooy, and D. Bouziou, "Earthquake Response of Underground Pipeline Networks in Christchurch, NZ," *Earthq. Spectra*, vol. 30, no. 1, pp. 183–204, Feb. 2014.

[8] BBC, "Holborn underground fire: Electrical fault caused 36-hour blaze," 2015. [Online]. Available: http://www.bbc.co.uk/news/uk-england-london-32231725. [Accessed: 04-May-2018].

[9] S. M. Rinaldi, J. P. Peerenboom, and T. K. Kelly, "Identifying, Understanding, and Analyzing Critical Infrastructure Interdependencies," *IEEE Control Syst. Mag.*, vol. 21, no. 6, pp. 11–25, Dec. 2001.

[10] S. Hosseini, K. Barker, and J. E. Ramirez-Marquez, "A review of definitions and measures of system resilience," *Reliab. Eng. Syst. Saf.*, vol. 145, pp. 47–61, 2016.

[11] R. Zimmerman, "Social Implications of Infrastructure Network Interactions," *J. Urban Technol.*, vol. 8, no. 3, pp. 97–119, Dec. 2001.

[12] D. D. Dudenhoeffer, M. R. Permann, and C. Miller, "Interdependency Modeling and Emergency Response," in *Proceedings of the 2007 Summer Computer Simulation Conference*, 2007, pp. 1230–1237.

[13] A. Volkanovski, M. Čepin, and B. Mavko, "Application of the fault tree analysis for assessment of power system reliability," *Reliab. Eng. Syst. Saf.*, vol. 94, no. 6, pp. 1116–1127, 2009.

[14] H.-S. J. Min, W. Beyeler, T. Brown, Y. J. Son, and A. T. Jones, "Toward modeling and simulation of critical national infrastructure interdependencies," *IIE Trans.*, vol. 39, no. 1, pp. 57–71, Jan. 2007.

[15] C. Nan and G. Sansavini, "A quantitative method for assessing resilience of interdependent infrastructures," *Reliab. Eng. Syst. Saf.*, vol. 157, pp. 35–53, 2017.

[16] Y. Y. Haimes and P. Jiang, "Leontief-Based Model of Risk in Complex Interconnected Infrastructures," *J. Infrastruct. Syst.*, vol. 7, no. 1, pp. 1–12, 2001.

[17] L. Dueñas-Osorio, J. Craig, and B. Goodno, "Seismic response of critical interdependent networks," *Earthq. Eng. Struct. Dyn.*, vol. 36, pp. 285–306, 2007.

[18] E. E. Lee II, J. E. Mitchell, and W. A. Wallace, "Restoration of Services in Interdependent Infrastructure Systems: A Network Flows Approach," *IEEE Trans. Syst. Man, Cybern. Part C Appl. Rev.*, vol. 37, no. 6, pp. 1303–1317, Nov. 2007.

[19] S. Buldyrev, R. Parshani, G. Paul, H. E. Stanley, and S. Havlin, "Catastrophic cascade of failures in interdependent networks," *Nature*, vol. 464, pp. 1025–8, 2010.

[20] R. Holden, D. V. Val, R. Burkhard, and S. Nodwell, "A network flow model for interdependent infrastructures at the local scale," *Saf. Sci.*, vol. 53, pp. 51–60, 2013.

[21] R. M. D'Souza, C. D. Brummitt, and E. A. Leicht, "Modeling Interdependent Networks as Random Graphs: Connectivity and Systemic Risk," in *Networks of Networks: The Last Frontier of Complexity*, G. D'Agostino and A. Scala, Eds. Cham: Springer, 2014.

[22] J. G. Jin, L. C. Tang, L. Sun, and D. H. Lee, "Enhancing metro network resilience via localized integration with bus services," *Transp. Res. Part E Logist. Transp. Rev.*, vol. 63, pp. 17–30, 2014.

[23] H. Fotouhi, S. Moryadee, and E. Miller-Hooks, "Quantifying the Resilience of an Urban Traffic-Electric Power Coupled System," *Reliab. Eng. Syst. Saf.*, vol. 163, pp. 79–94, 2017.

[24] S. Thacker, R. Pant, and J. W. Hall, "System-of-systems formulation and disruption analysis for multi-scale critical national infrastructures," *Reliab. Eng. Syst. Saf.*, vol. 167, no. January 2015, pp. 30–41, 2017.

[25] M. Ouyang, "Review on modeling and simulation of interdependent critical infrastructure systems," *Reliab. Eng. Syst. Saf.*, vol. 121, pp. 43–60, 2014.

[26] M. Iturriza, L. Labaka, J. M. Sarriegi, and J. Hernantes, "Modelling methodologies for analysing critical infrastructures,"

J. Simul., vol. 12, no. 2, pp. 128–143, 2018.

[27] E. Zio, "Challenges in the vulnerability and risk analysis of critical infrastructures," *Reliab. Eng. Syst. Saf.*, vol. 152, pp. 137–150, 2016.

[28] P. Hines, E. Cotilla-Sanchez, and S. Blumsack, "Do topological models provide good information about electricity infrastructure vulnerability?," *Chaos*, vol. 20, no. 3, Sep. 2010.

[29] M. Ouyang, "Comparisons of purely topological model, betweenness based model and direct current power flow model to analyze power grid vulnerability.," *Chaos*, vol. 23, no. 2, Jun. 2013.

[30] M. Ouyang, L. Zhao, L. Hong, and Z. Pan, "Comparisons of complex network based models and real train flow model to analyze Chinese railway vulnerability," *Reliab. Eng. Syst. Saf.*, vol. 123, pp. 38–46, Mar. 2014.

[31] M. Ouyang, "Critical location identification and vulnerability analysis of interdependent infrastructure systems under spatially localized attacks," *Reliab. Eng. Syst. Saf.*, vol. 154, pp. 106–116, 2016.

[32] A. Azzolin, L. Dueñas-Osorio, F. Cadini, and E. Zio, "Electrical and topological drivers of the cascading failure dynamics in power transmission networks," *Reliab. Eng. Syst. Saf.*, vol. 175, no. March, pp. 196–206, 2018.

[33] W. Sun, P. Bocchini, and B. D. Davison, "Resilience metrics and measurement methods for transportation infrastructure : the state of the art," *Sustain. Resilient Infrastruct.*, vol. 9689, pp. 1–33, 2018.

[34] M. Bruneau, S. E. Chang, R. T. Eguchi, G. C. Lee, T. D. O'Rourke, A. M. Reinhorn, M. Shinozuka, K. Tierney, W. a. Wallace, and D. von Winterfeldt, "A Framework to Quantitatively Assess and Enhance the Seismic Resilience of Communities," *Earthq. Spectra*, vol. 19, no. 4, pp. 733–752, Nov. 2003.

[35] M. Ouyang, L. Dueñas-Osorio, and X. Min, "A three-stage resilience analysis framework for urban infrastructure systems," *Struct. Saf.*, vol. 36–37, no. 0, pp. 23–31, 2012.

[36] P. Angeloudis and D. Fisk, "Large subway systems as complex networks," *Phys. A Stat. Mech. its Appl.*, vol. 367, pp. 553–558, 2006.

[37] A. M. Caunhye, Y. Zhang, M. Li, and X. Nie, "A location-routing model for prepositioning and distributing emergency supplies," *Transp. Res. Part E Logist. Transp. Rev.*, vol. 90, pp. 161–176, 2016.

[38] W. Zhang, N. Wang, and C. Nicholson, "Resilience-based post-disaster recovery strategies for road-bridge networks," *Struct. Infrastruct. Eng.*, vol. 13, no. 11, pp. 1404–1413, 2017.

[39] L. Faramondi, R. Setola, S. Panzieri, F. Pascucci, and G. Oliva, "Finding critical nodes in infrastructure networks," *Int. J. Crit. Infrastruct. Prot.*, vol. 20, pp. 3–15, 2018.

[40] C. D. Nicholson, K. Barker, and J. E. Ramirez-Marquez, "Flow-based vulnerability measures for network component importance: Experimentation with preparedness planning," *Reliab. Eng. Syst. Saf.*, vol. 145, pp. 62–73, Jan. 2016.

[41] D. L. Alderson, G. G. Brown, and W. M. Carlyle, "Assessing and Improving Operational Resilience of Critical Infrastructures and Other Systems," in *INFORMS 2014 Tutorials in Operations Research*, 2014, no. November.

[42] P. Trucco, E. Cagno, and M. De Ambroggi, "Dynamic functional modelling of vulnerability and interoperability of Critical Infrastructures," *Reliab. Eng. Syst. Saf.*, vol. 105, pp. 51–63, Sep. 2012.

[43] L. Chen and E. Miller-Hooks, "Resilience: An Indicator of Recovery Capability in Intermodal Freight Transport," *Transp. Sci.*, vol. 46, no. 1, pp. 109–123, 2012.

[44] P. Chopade and M. Bikdash, "New centrality measures for assessing smart grid vulnerabilities and predicting brownouts and blackouts," *Int. J. Crit. Infrastruct. Prot.*, vol. 12, pp. 29–45, 2014.

[45] R. Faturechi and E. Miller-Hooks, "Travel time resilience of roadway networks under disaster," *Transp. Res. Part B Methodol.*, vol. 70, pp. 47–64, 2014.

[46] M. Nogal, A. O'Connor, B. Caulfield, and B. Martinez-Pastor, "Resilience of Traffic Networks: From Perturbation to Recovery via a Dynamic Restricted Equilibrium Model," *Reliab. Eng. Syst. Saf.*, vol. 156, pp. 84–96, 2016.

[47] O. Cats, G. J. Koppenol, and M. Warnier, "Robustness assessment of link capacity reduction for complex networks: Application for public transport systems," *Reliab. Eng. Syst. Saf.*, vol. 167, no. July, pp. 544–553, 2017.

[48] J. C. Lam, M. Heitzler, J. Hackl, and B. T. Adey, "Modelling the functional capacity losses of networks exposed to hazards," *Sustain. Resilient Infrastruct.*, vol. 9689, no. May, pp. 1–19, 2018.

[49] O. Cats and E. Jenelius, "Planning for the unexpected: The value of reserve capacity for public transport network robustness," *Transp. Res. Part A Policy Pract.*, vol. 81, pp. 47–61, 2015.

[50] M. K. Miller and J. W. Baker, "Coupling mode-destination accessibility with seismic risk assessment to identify at-risk communities," *Reliab. Eng. Syst. Saf.*, vol. 147, pp. 60–71, 2015.

[51] G. P. Cimellaro, A. M. Reinhorn, and M. Bruneau, "Framework for analytical quantification of disaster resilience," *Eng. Struct.*, vol. 32, no. 11, pp. 3639–3649, 2010.

[52] M. Fonoberova, "Optimal Flows in Dynamic Networks and Algorithms for their Finding," in *Handbook of Optimization in Complex Networks: Theory and Applications*, M. T. Thai and P. M. Pardalos, Eds. Boston, MA: Springer US, 2012, pp. 363–403.

[53] R. K. Ahuja, T. L. Magnanti, and J. B. Orlin, *Network Flows: Theory, Algorithms, and Applications*. Prentice Hall, 1993.

[54] J. Y. Yen, “Finding the K Shortest Loopless Paths in a Network,” *Manage. Sci.*, vol. 17, no. 11, pp. 712–716, 1971.

[55] UK Power Networks PLC, “Long Term Development Statement,” 2017. [Online]. Available: https://www.ukpowernetworks.co.uk/internet/en/about-us/regulatory-information/long-term-development-statement.html.

[56] Transport for London, “Rolling Origin and Destination Survey,” 2016. [Online]. Available: https://tfl.gov.uk/info-for/open-data-users/. [Accessed: 04-May-2018].

[57] London Borough of Brent, “Strategic Flood Risk Assessment (SFRA) Level 1,” 2007. [Online]. Available: http://geosmartinfo.co.uk/wp-content/uploads/sfra/Strategic-flood-report-2007.pdf. [Accessed: 04-May-2018].

[58] London Borough of Brent, “Flood Risk Management Strategy: Managing the Floods Risk in Brent,” 2015. [Online]. Available: https://www.brent.gov.uk/media/16406897/flood-risk-strategy-sept-2015.pdf. [Accessed: 04-May-2018].

[59] “London Underground Track and Traction Current,” 2000. [Online]. Available: http://www.trainweb.org/tubeprune/tractioncurr.htm. [Accessed: 04-May-2018].

[60] London Economics, “The Value of Lost Load (VoLL) for Electricity in Great Britain: Final report for OFGEM and DECC,” 2013. [Online]. Available: https://www.ofgem.gov.uk/ofgem-publications/82293/london-economics-value-lost-load-electricity-gbpdf. [Accessed: 04-May-2018].

[61] Transport for London, “Unified API.” [Online]. Available: https://api.tfl.gov.uk/. [Accessed: 04-May-2018].

[62] Transport for London, “FOI-0175-1314: Station to Station Journey Times,” 2013. [Online]. Available: https://www.whatdotheyknow.com/request/station_to_station_journey_times. [Accessed: 04-May-2018].

[63] Transport for London, “FOI-1216-1112: Gate-to-platform and interchange walking times,” 2012. [Online]. Available: https://www.whatdotheyknow.com/request/gate_to_platform_and_interchange. [Accessed: 04-May-2018].

[64] UK Department for Transport, “Provision of market research for value of travel time savings and reliability,” 2015. [Online]. Available: https://www.gov.uk/government/publications/values-of-travel-time-savings-and-reliability-final-reports. [Accessed: 04-May-2018].

[65] Carto Metro, “Detailed map of London Tube, Underground, Overground, DLR, Tramlink & National Rail,” 2017. [Online]. Available: http://carto.metro.free.fr/metro-london/. [Accessed: 04-May-2018].

[66] Transport for London, “TfL Energy Purchasing 2020 to 2023,” 2017. [Online]. Available: http://content.tfl.gov.uk/fc-20171205-part-1-item08-tfl-energy-purchasing-2020-2023.pdf. [Accessed: 04-May-2018].

APPENDIX

Table 4 Infrastructure systems, components and parameters

System	Component	Parameter	Value / description	Data sources	Assumptions
LPN	Nodes	V^{SC}	1,379 nodes including: 1,294 busbars (voltage levels 11 to 132 kV), 6 bulk supply points for traction power, 79 traction power supply substations	UKPN LTDS [55] Trainweb [59]	
		$\hat{g}_i^t$	Rated capacity of 67 super-grid transformers	UKPN LTDS [55]	
	Links	E^{SC}	1,742 links including: 828 connectors, 394 two-winding transformers, 80 three-winding transformers, reverse direction links where applicable	UKPN LTDS [55]	
		$\hat{f}_{i,j}^t$	Cables and transformers: rated capacity Intra-substation connectors: unlimited	UKPN LTDS [55]	
	Assets	A	392 assets including: 19 grid supply points, 247 high-voltage substations, 126 low-voltage substations	UKPN LTDS [55]	
	Demand	$\check{u}_i^t$	Load profiles for 128 demand nodes derived from peak demand and minimum load scaling factor	UKPN LTDS [55]	A 1
		v_i^{SC}	16,940 GBP/MWh (weighted average value of lost load for peak winter workdays in the UK)	London Econ. [60]	A 2
LPN repair	Nodes	V^{SC}	12 engineering depots, 392 potential repair sites	UKPN LTDS [55]	
		$\hat{g}_i^t$	Engineering depots: 1 repair resource units per hour		A 3
	Links	E^{SC}	784 repair resource deployment links		A 4
		$\hat{f}_{i,j}^t$	0.25 if distance is less than 10 km 0.20 if distance is between 10 and 25 km 0.17 if distance is greater than 25 km		A 5
LUN	Nodes	V^{MC}	1,045 nodes including: 267 stations, 778 platforms	TfL RODS [56]	
	Links	E^{MC}	2,315 links including: 759 on-train links, 778 boarding links, 778 alighting links	TfL RODS [56]	
		$\hat{f}_{i,j}^t$	On-train-links: Number of scheduled train departures per hour multiplied with rolling stock capacity Boarding and alighting links: capacity estimated based on maximum station entries and exits	TfL API [61]	A 6
		$c_{i,j}^{\mathrm{f}}$	On-train-links: station-to-station journey times Alighting links: platform-to-ticket-hall walking time Boarding links: ticket-hall-to-platform walking time plus average waiting time for first train All travel times valued at 11.21 GBP/h	TfL FOIs [62], [63] TfL API [61] DfT VoTT [64]	A 7
	Assets	A	389 assets including: 267 stations, 79 track sections, 8 line control systems, 8 rolling stock fleets, 8 control centres, 19 depots	TfL RODS [56] Trainweb [59] Carto Metro [65]	
	Demand	$\check{f}_{o,d}^t$	Travel demand profiles for 32,109 OD pairs	TfL RODS [56]	A 8
		$v_{o,d}^{\mathrm{MC}}$	Cost of alternative transport modes estimated based on geographic distance		A 9
LUN repair	Nodes	V^{SC}	19 engineering depots, 373 potential repair sites	Carto Metro [65]	
		$\hat{g}_i^t$	Engineering depots: 1 repair resource units per hour		A 3
	Links	E^{SC}	957 repair resource deployment links		A 4
		$\hat{f}_{i,j}^t$	0.25 if distance is less than 10 km 0.20 if distance is between 10 and 25 km 0.17 if distance is greater than 25 km		A 5

Table 5 Dependency relations

Dependency type	From	To	No. of instances	Parameters	Assumptions
Failure propagation	Flood hazard	Assets in flood zone 1	9	$p_{h,k} = 0.250$ $t_{h,k} = 0$	A 10
	Flood hazard	Assets in flood zone 2	30	$p_{h,k} = 0.050$ $t_{h,k} = 1$	A 10
	Asset $k \in A$	Assets located less than 100 m from k	1,598	$p_{h,k} = 0.250$ $t_{h,k} = 0$	A 11
	Asset $k \in A$	Assets located between 100 and 1,000 m from k	5,940	$p_{h,k} = 0.050$ $t_{h,k} = 1$	A 11
Asset utilisation	Electricity substation assets k	Supply nodes located at k and links starting or ending at k	4,837		
	Metro station asset k	Boarding and alighting links of k	1,556		
	Track section asset k	On-train links that use k	759		
Logic	Line control assets	Track section assets	79		
	Rolling stock fleet assets	Track section assets	79		
	Control centre assets	Line control assets	10		
	Depot assets	Rolling stock fleet assets	20		
Input	Low-voltage electricity substation node	Metro station asset	534	$\alpha_{i,k}^{\mathrm{U}} = 0.10$	A 12
	Traction power supply substation node	Track section assets	79	$\alpha_{i,k}^{\mathrm{U}} = 4.00$	A 13
	Potential repair site node	Asset	765	$\alpha_{i,k}^{\mathrm{R}} = 1.00$	A 14

1 *Table 6 Overview of modelling assumptions*

No.	System	Assumption	Justification
A 1	LPN	Time series of substation loads can be estimated by fitting a generic load profile to the peak and minimum load available from the UKPN LTDS [55].	Standard method used in the absence of time series load data
A 2	LPN	The weighted average value of lost load specified in London Economics [60] as 16,940 GBP/MWh applies to all demand nodes.	Best available estimate for economic cost of power outages
A 3	LPN repair & LUN repair	Each engineering depot can dispatch 1 units of repair resources per time step.	Sensitivity analysis provided
A 4	LPN repair & LUN repair	Depots can be repaired by local engineering teams, control centre assets can be repaired by engineering teams from any depot, track sections can be repaired by the depot belonging to the respective line, metro stations and electricity substations can be repaired by the two nearest depots.	Estimate based on subject matter expertise
A 5	LPN repair & LUN repair	The time to repair an asset is determined by the distance from the engineering depot carrying out the repair (4 hours if less than 10 km, 5 hours if between 10 and 25 km, 6 hours if greater than 25 km).	Estimate based on subject matter expertise
A 6	LUN	Boarding and alighting links have an excess capacity of 10 % with respect to the maximum station entries or exits recorded in [56] but not less than 5,000 passengers per hour.	Most metro stations in central London are near capacity during peak hours
A 7	LUN	All passengers value travel time at 11.21 GBP/h.	Assumption necessary due to the unavailability of trip purpose data
A 8	LUN	Time series of travel demands can be estimated by distributing travel demand given in TfL RODS [56] for 6 daily time slots uniformly within the respective time slot and calculating the moving average over three hours.	Standard smoothing method for demand forecasting
A 9	LUN	The value of the transportation services provided can be estimated as: $5\ \mathrm{GBP} + \frac{\text{Distance in km}}{5\frac{\mathrm{km}}{\mathrm{h}}} \times 11.21\frac{\mathrm{GBP}}{\mathrm{h}}$	The relatively high value is justified because in the case of major disruptions the cost of alternative transport modes is likely to be above average, e.g. due to congestion
A 10	LPN & LUN	Assets located less than 2,000 m from the reservoir suffer flood damage with a probability of 33 % and no time lag. Assets located at a distance between 2,000 and 4,000 m are damaged with a probability of 10 % and a time lag of 1 hour.	Hypothetical flood risk exposure
A 11	LPN & LUN	Failure propagates between assets located less than 100 m apart with a probability of 33 % and no time lag, and between assets located between 100 and 1,000 m apart with a probability of 5 % and a time lag of 1 hour.	Hypothetical failure propagation risk exposure
A 12	LPN & LUN	Metro stations require a power supply of 0.1 MW when used at full capacity.	Estimate based on dividing London Undergrounds total non-traction power consumption of 200 GWh/a [66] by the number of stations and assuming a peak-to-average ratio of 1.2
A 13	LPN & LUN	Track sections require a power supply of 4.0 MW when being used at full capacity.	Estimate based on dividing London Undergrounds total traction power consumption of 1,363 GWh/a [66] by the number of track sections and assuming a peak-to-average ratio of 2.0
A 14	LPN & LUN	Failed asset requires 1 unit of repair resources to be fully repaired.	Based on the assumption that all flood damage incidents are of similar magnitude

2